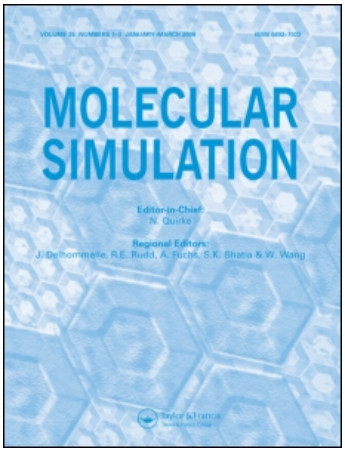

Molecular Simulation
Publication details, including instructions for authors and subscription information:
http://www.informaworld.com/smpp/title~content=t713644482

Correlated movements of ions and water in a nanochannel

M. Haan[a]; J. F. Gwan[a]; A. Baumgaertner[a]
[a] Institut für Festkörperforschung, Forschungszentrum Jülich, Jülich, Germany

First published on: 21 September 2010

To cite this Article Haan, M. , Gwan, J. F. and Baumgaertner, A.(2009) 'Correlated movements of ions and water in a nanochannel', Molecular Simulation, 35: 1, 13 — 23, First published on: 21 September 2010 (iFirst)
To link to this Article: DOI: 10.1080/08927020802433160
URL: http://dx.doi.org/10.1080/08927020802433160

Molecular Simulation
Vol. 35, Nos. 1–2, January–February 2009, 13–23

Taylor & Francis
Taylor & Francis Group

Correlated movements of ions and water in a nanochannel

M. Haan, J.F. Gwan[1] and A. Baumgaertner*

Institut für Festkörperforschung, Forschungszentrum Jülich, Jülich, Germany

(*Received 6 June 2008; final version received 25 August 2008*)

We have studied the molecular mechanism of the ion transport in a long channel (≈ 70 Å) filled with an alternating sequence of ions and water molecules at various densities. The molecular structure of the channel was adopted from the structure of the selectivity pore of the KcsA potassium channel. The results from molecular dynamics simulations show that the ion conductivity is based on a fine-tuned interplay between the three constituents of the channel: the ions, the water molecules and the flexible carbonyl groups of the channel's backbone, which represent a one-dimensional fluctuating lattice potential for ions and water. The unidirectional transport is based on the hopping processes of bound ion–water pairs mediated by the lattice potential. The cooperativity of the transport is deduced from the observations that isolated ion–water pairs, and isolated ions in a water-free channel, do not perform long-ranged movements. It is suggested that the water molecules cause a rectification of the movements of ion–water pairs at high densities.

Keywords: potassium channel; permeation; ion conduction; molecular dynamics simulation; incommensurability; ratchet; rectification

1. Introduction

Correlated motions are considered to be of a great challenge to realise and develop because such motions require concerted displacements of multiple components within a tightly condensed medium. One example is the transport of microscopic particles, including atoms, ions, molecules and colloids, through nanochannels, which is significant for fundamental biological processes and industrial applications as well. Examples include molecular or ionic permeation in zeolites [1,2], carbon nanotubes [3,4], aquaporins [5] and ion channels [6–8]. In the present paper, we report on molecular dynamics (MD) studies of the microscopic non-equilibrium transport of ions and water molecules through a nanochannel that shares structural similarities with a known biological potassium channel [9,10].

Potassium ion channels reside in cell membranes and they work by selecting specific ions and by catalysing the passive diffusion through the selectivity filter. The selectivity filter facilitates the diffusion of ions at rates approaching 10^8 ions per second under physiological electrochemical gradients [11]. Several decades ago, it was suggested that this high throughput rate was due to the 'multi-ion permeation process': the permeating ions line up in the narrow channel pore and move in a single file through the channel [12], which was believed to be a universal feature of the ion transportation process in potassium channels [11]. The multi-ion concept has been assumed to be valid; its molecular mechanism, however, has remained obscure. Recent MD simulations [7,13–16] of atomic models of the KcsA ion channel [9,10] have contributed significantly to the details of permeation and selectivity processes [17,18]. However, a clear picture of the details of the concerted movements of ions and water remained elusive, because the simulation times were limited to less than tens of nanoseconds, which is of the order of one exciting ion on average. In addition, significant finite size effects due to the short length of the selectivity filter (≈ 12 Å) have prohibited developing a basic physical concept for ion permeation. In this situation, following a common approach in statistical physics, we have studied a model of a nanochannel, which shares the essential molecular details of the pore of the KcsA channel, and is a finite periodic continuation of the original selectivity filter. Whether such a nanochannel of approximately 70 Å can be constructed under laboratory conditions is still a matter of speculation. In particular, the question of stability in a lipid multilayer system or the embedding of the nanochannel in a solid or soft matter matrix has not yet been addressed. Therefore, the presented results and discussions below may be considered as predictions that can be compared with other one-dimensional transport systems as there are superionic conductors [19–24] and other nanotubes [3,4,25,26]. Since the ion conduction of the present peptide nanochannel is probably of the same magnitude as that of the KcsA channel, it would not be a surprise if its transport properties would be superior to that of ceramic

*Corresponding author. Email: a.baumgaertner@fz-juelich.de

ISSN 0892-7022 print/ISSN 1029-0435 online

DOI: 10.1080/08927020802433160
http://www.informaworld.com

superionic conductors. The present study is a continuation of previous studies on the KcsA channel [27] and a peptide nanochannel [28], where the latter was based on a different modelling approach as employed in the present study.

2. Model and simulation method

2.1 The model of the nanochannel

We have constructed an atomic model of the extended selectivity filter (nanochannel) of the potassium channel KcsA. The atomic coordinates for this nanochannel were taken from the crystallographic structure of the KcsA potassium channel resolved by X-ray diffraction method at high resolutions [9,10]. The channel protein is a tetramer composed of four identical monomers, and each monomer contains 160 amino residues. Only the membrane part of the channel (residues 23–119) was resolved in the experiments. This type of model system has been used recently in several MD simulations [14,15,27] where the protein was embedded in a fully hydrated lipid bilayer membrane. In the present work, we are only interested in the selectivity filter of the ion channel. The selectivity filter is the central structural element of the KcsA channel and is depicted in Figure 1. The filter consists of four strands of the sequence Thr, Val, Gly, Tyr and Gly (TVGYG). They are arranged with their carbonyl oxygen atoms pointing inwards towards the ion conduction pathway. This arrangement creates four potential ion-binding sites into which a K^+ can be bound surrounded by eight oxygen atoms from the surrounding carbonyls.

The nanochannel (Figure 2) is constructed by a finite continuation of the original KcsA selectivity filter [28].

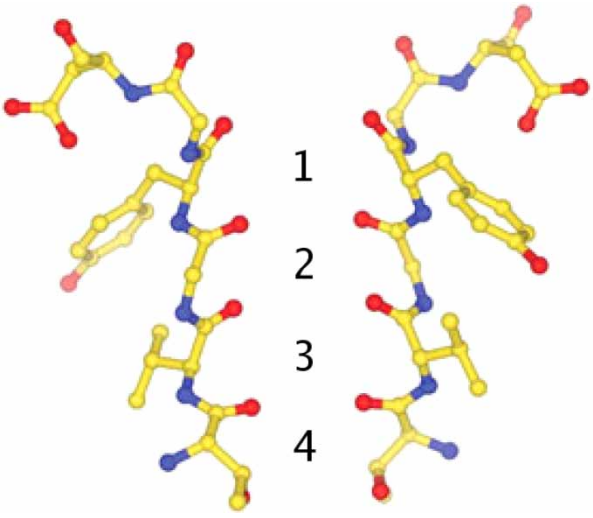

Figure 1. Structure of selectivity pore of the KcsA potassium channel [9,10]. Only two of the tetrameric proteins are shown. The red tips represent the carbonyl oxygen atoms and the blue nitrogen atoms.

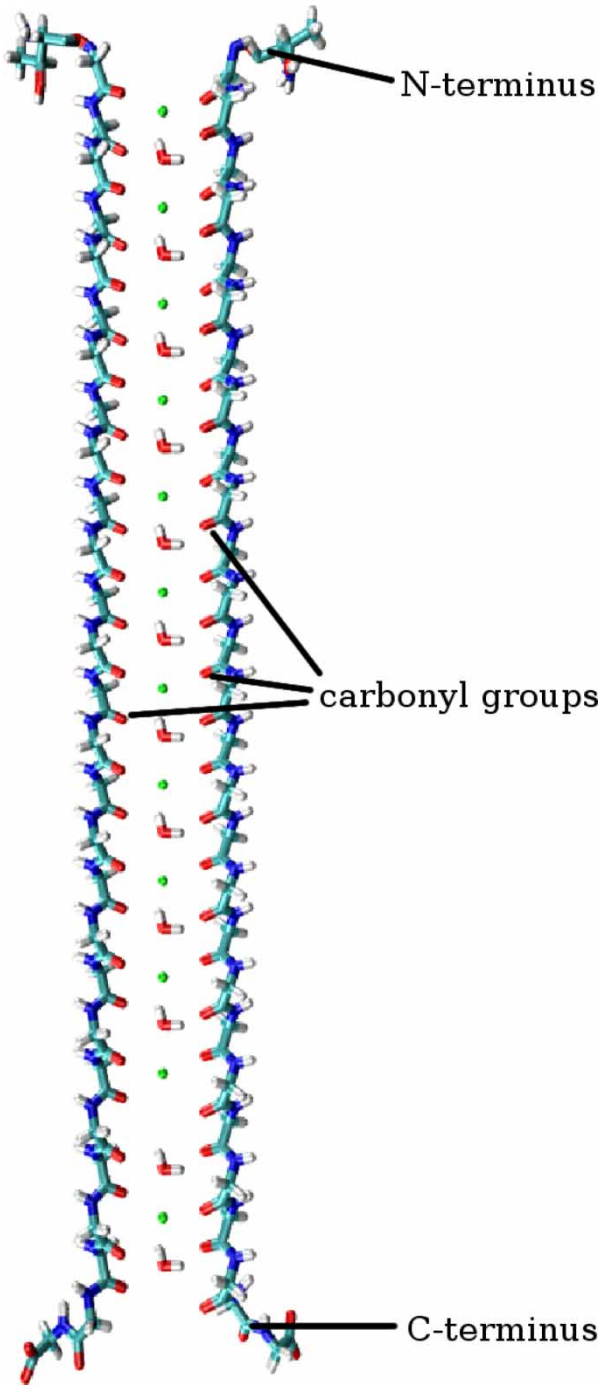

Figure 2. Molecular model of the extended ion channel constructed as a periodically continued KcsA selectivity filter. The channel contains an alternating sequence of ions and water molecules.

We used the peptide Val76-Gly77 as the basic unit and built a nanochannel, made of the basic unit, containing 25 binding sites. All residues of the nanochannel were replaced by glycine. At each binding site, an ion or a water molecule is stably coordinated by eight carbonyl oxygens, four on each side. The width of such a binding site along

the channel axis is about 3 Å. The periodicity of the binding sites represents a one-dimensional lattice potential provided by the carbonyl groups of the backbone. According to experimental findings [9,10,29], we assume that the nanochannel contains potassium ions and water molecules. Figure 2 shows as an example the alternating sequence of ions and water. For the water molecule, we employed the TIP3P model, a rigid three-charge model [30], which has the charges -0.834 and $+0.417$, for oxygen and hydrogen, respectively. The carbonyl group is modelled as a polar group (Figure 3) where its oxygen end is negatively charged, -0.5 electron units, and the connecting carbon atom is positively charged, 0.62 electron units [31]. Because the total charge of a carbonyl group is slightly positive, $+0.12$, the electrostatic interaction at large distances between a single potassium ion and a carbonyl group is slightly repulsive. The backbone atoms (N, C_α, C) and the last ion and water molecule (at the top and bottom in Figure 2) were restrained at their positions by harmonic forces with force constant 2.0 kcal/mol Å^2. The restraints of the backbone atoms are necessary in order to provide a certain rigidity of the one-dimensional structure. Under experimental conditions, this could be thought to be provided by an external embedding matrix of a comparable rigidity. It has been shown [32] that weaker restraints, which lead to higher flexibility of the peptide backbone and larger tube diameter, yields a disappearance of the concerted ion conduction as reported below. The width of the channel, represented by the distance of the C atoms of opposite backbones, is 7 Å. Most of the simulation parameters are listed in Table 1. The employed cut-off value is larger than the system, meaning that there is effectively no cut-off. Other default parameters are listed in the AMBER8 manual.

2.2 *Simulation methods*

The simulation was carried out using the AMBER9.0 program [31]. The equations of motion were integrated using the Verlet leapfrog algorithm. The equations of motion were integrated with a time step of 2 fs. The atomic coordinates were saved every 1 ps and the velocity every 10 ps. The temperature was kept at 300 K by applying the Berendsen coupling algorithm on the temperature scaling [33]. The SHAKE constraint algorithm was employed to remove the stretching freedom of all bonds involving hydrogens. The 1–4 van der Waals and the 1–4 electrostatic interactions (van der Waals/electrostatic interactions separated by only three covalent bonds) were both scaled [34] by the factor 2.0. The translational and rotational centre-of-mass motion was removed every 1000 steps. This is the default value. For the present study, we employed an implicit solvent model rather than an explicit model, as used previously [27], for the simulation of the KcsA channel, where lipid and water molecules were included explicitly. Also, the inclusion of an implicit solvent in the calculation is an improvement when compared with previous studies on the nanochannel [28], where the nanochannel was embedded in vacuum. We chose the generalised Born implicit solvent model, employing a modified version of the GB^{OBC} model [35], to simulate the effect of the hydrophobic part of the membrane on charge shielding by treating it as a fluid with a dielectric constant $\varepsilon = 2$ and a salt concentration of 0.2. The latter is the concentration of 1–1 mobile counterions in solution, using a modified GB theory based on the Debye–Hückel limiting law for ion screening of interactions [36]. It should be noted that the neutral state of the system is taken into account implicitly by the GB approach. The direct Coulomb interactions between the ions, water molecules and carbonyl groups are not screened.

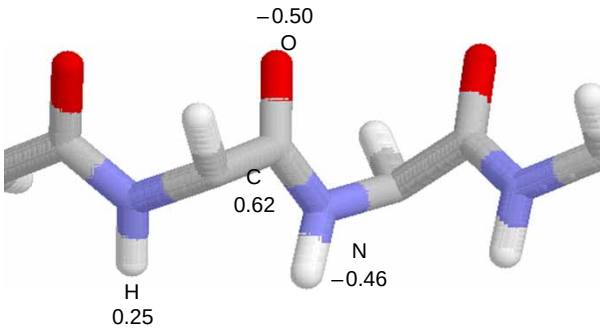

Figure 3. Charge distributions of the C (grey), O (red), N (blue) and H (white) atoms of the backbone in electron units.

Table 1. Some parameters used for the simulations.

Temperature	$T = 300$ K
Time constant for heat bath coupling to the system	$\tau_{tp} = 2.0$ ps
Collision frequency for Langevin dynamics	$\gamma_{ln} = 1.0\,ps^{-1}$
Dielectric constant	$\varepsilon = 2$
Force field cut-off value	120 Å
Integration time step	2 fs

2.3 *The potentials inside the nanochannel*

We have calculated the energy, $U(y)$, for one ion and water molecule along the channel axis y. We used an external dielectric constant of $\varepsilon = 2$ and no cut-off distance. The energy was calculated in the same way as in the simulation protocol, but here a single ion or water molecule was placed at various positions along the static (frozen) channel in its initial conformation. Of course, this potential is not exactly the same as experienced by ions and water during MD simulations, e.g. measured by the potential of mean force, but rather serves as a first approximation.

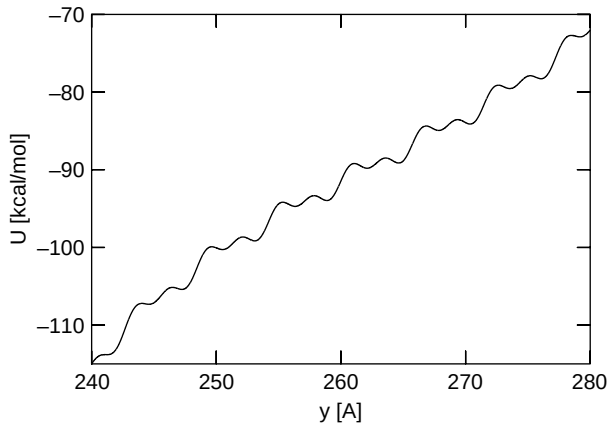

Figure 4. The potential for one potassium ion in the static nanochannel.

The energy profiles are depicted in Figures 4 and 5 for ions and water, respectively. The potential gradient towards the N-terminus for potassium ions in the channel is a result of the electric field between C- and N-termini. The potentials have a depth of about 1–5 kcal/mol for both ions and water molecules, although the detailed form of the potentials differs in both cases. The potential profile for a water molecule depends significantly on its orientation Ω. The orientation of the water molecule, Ω, with respect to the channel axis (along the *y*-axis) is defined as

$$\Omega = \frac{y_O - (y_{H1} + y_{H2})/2}{|r_O - (r_{H1} + r_{H2})/2|}, \tag{0.1}$$

which is the difference in the *y*-coordinates of the oxygen atom, y_O, and the centre of mass of the hydrogen atoms, H1 and H2, divided by the distances *r*.

2.4 The driving force

Since the potential barriers for the ion (Figure 4) are of the order of $2-8\,k_BT$, a driving force is needed for the conduction of the ions through the channel. This is achieved by introducing a certain numbers of unoccupied binding sites (vacancies) in the channel, which can break the symmetry between the periodicity of the lattice potential and the inter-ionic Coulomb repulsion. Similar to the studies on the Frenkel–Kontorova model [19–24,37], we will use the term 'commensurable' for ion configurations in which the equilibrium distance of the potassium ions coincides with the periodicity of the lattice potential. In this case, without any other influences, the ions would rest exactly in the energetic minima (binding sites) of the lattice potential. Figure 6 shows three different configurations, two with a commensurable occupation and one which is incommensurable. The commensurability can be characterised by a density number ν, the 'ion occupation number', which is defined as

$$\nu = \frac{\text{number of binding sites} - 1}{\text{number of ions} - 1}. \tag{0.2}$$

The relevant binding sites are those between and including the sites occupied by the two outermost ions. For commensurable ion distributions, the number is an integer. Note that this value is only relevant for configurations holding at least three ions, as fewer would automatically be commensurable regardless of the number of sites. For one ion the value is not defined, while for two ions it is always an integer. For more ions, and assuming that there is always a maximum of one ion per site, ν, is always greater or equal 1.

Incommensurable conditions induce a driving force that causes random jumps among the binding sites. Examples of commensurable and incommensurable conditions are illustrated in Figure 7(a),(b), respectively. The example shown in Figure 7(b) resembles the situation illustrated in Figure 2. The channel in Figure 7(b) is fully occupied by ions and water except the fourth binding site from the right, S_4. The ion next to the vacancy at S_5 experiences Coulomb forces from all other ions and water molecules in the nanochannel. Neglecting in a first approximation the contributions from the water molecules, the repulsive Coulomb force on this ion at S_5 is stronger from the left than from the right, because the main contribution comes from the nearest neighbour ion to the

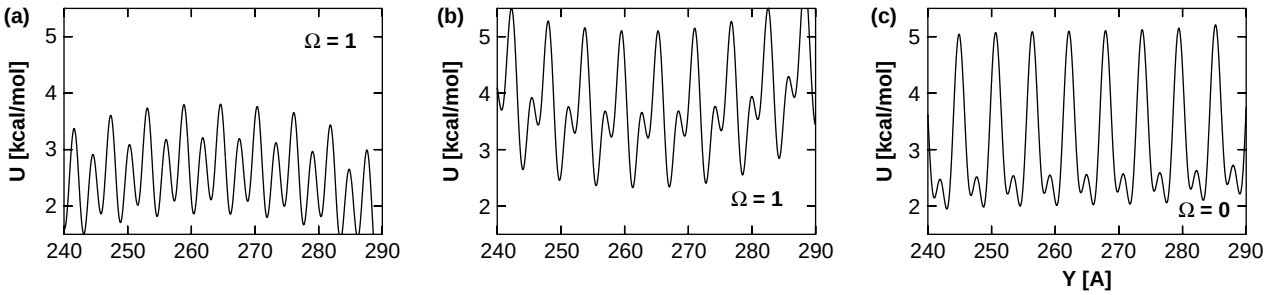

Figure 5. The potentials for one water molecule in the static nanochannel for three different orientations. (a) $\Omega = 1$, (b) $\Omega = -1$ and (c) $\Omega = 0$.

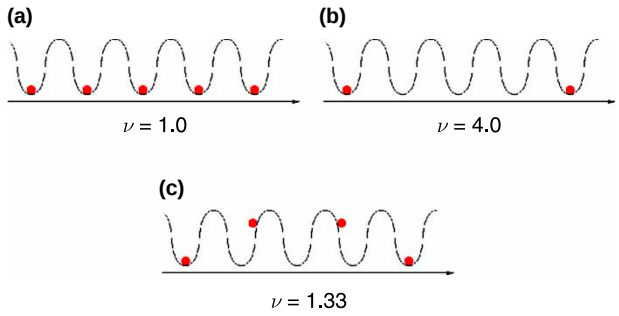

Figure 6. Schematic distributions of ions with varying density in a static periodic potential. In (a) and (b), the equilibrium distance of the ions coincides with the periodicity of the potential, so all ions rest inside these minima. In (c) these distances differ, forcing some ions out of the minima.

left, at site S_7, and the contribution of secondary importance from the ion at site S_2. Hence, the ion at S_5 has a tendency to move towards right and try to occupy the vacancy.

3. Results and discussion

We have studied the trajectories of ions and water in the channel at different conditions and for different configurations. In Sections 3.1 and 3.2, we consider the two situations where the channel contains either only water molecules or only potassium ions. The results from these simulations are then compared with the results presented in Sections 3.3 and 3.4, where correlations of ion–water pairs, at low and high densities, respectively, are presented and discussed.

3.1 Water-filled channel

In order to understand the correlated movements of ions and water in the channel, it is of interest to distinguish

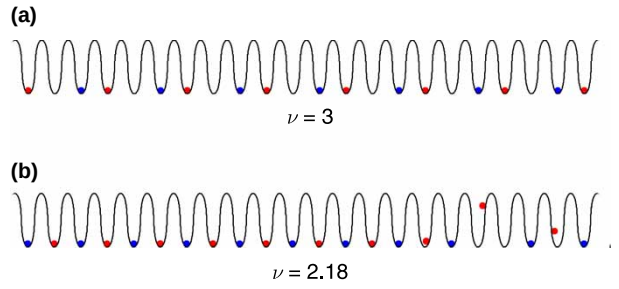

Figure 7. Schematic distributions of ions (red) and water molecules (blue) with varying density in a static periodic potential. In (a) the equilibrium distance of the ions coincides with the periodicity of the potential, so all ions rest inside these minima. In (b) these distances differ in the vicinity of the vacancy, forcing the ions nearby out of the minima. The water molecules are only shown for illustration, as they do not see the same potential as the ions do and are not subject to the same effects due to incommensurability.

correlated movements from the intrinsic movements of water alone. Therefore, we have simulated the channel filled with only water at high and low densities. The trajectories are shown in Figure 8. It should be noted that during the simulations the channel structure remains stable and no water molecules escaped from the channel. Figure 8(a) shows the trajectories of all water molecules at a high density, where almost all binding sites are occupied. It is observed that the water molecules move rather freely inside the channel and sometimes even occupy the same binding site. Obviously, the influence of the channel potential on the water molecules is rather weak. This is a consequence of the overall neutral charge of each water molecule. The interaction between the dipoles and the carbonyl groups, separating the binding sites, is not sufficient to induce significant correlated movements. The orientations of the water dipoles are essentially parallel after about 20 ps (Figure 9); all dipoles point towards the N-terminus with $\Omega \approx 1$. A significant

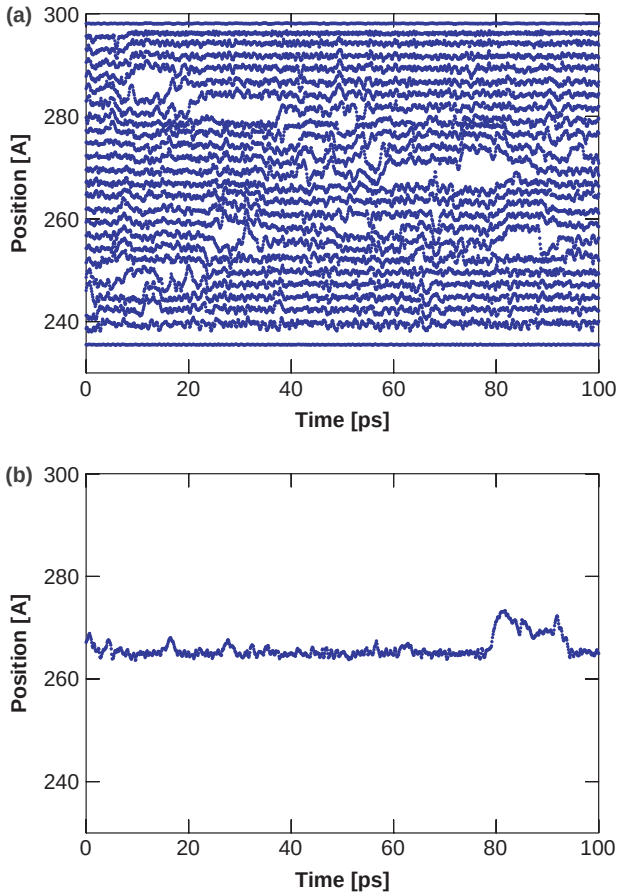

Figure 8. (a) Trajectories inside a channel that had one water molecule in each binding site except the one near the C-terminus at the beginning. The water molecules feel comparably little influence from one another and from the channel potential, allowing them to move rather freely. (b) The trajectory of one single water molecule in the channel.

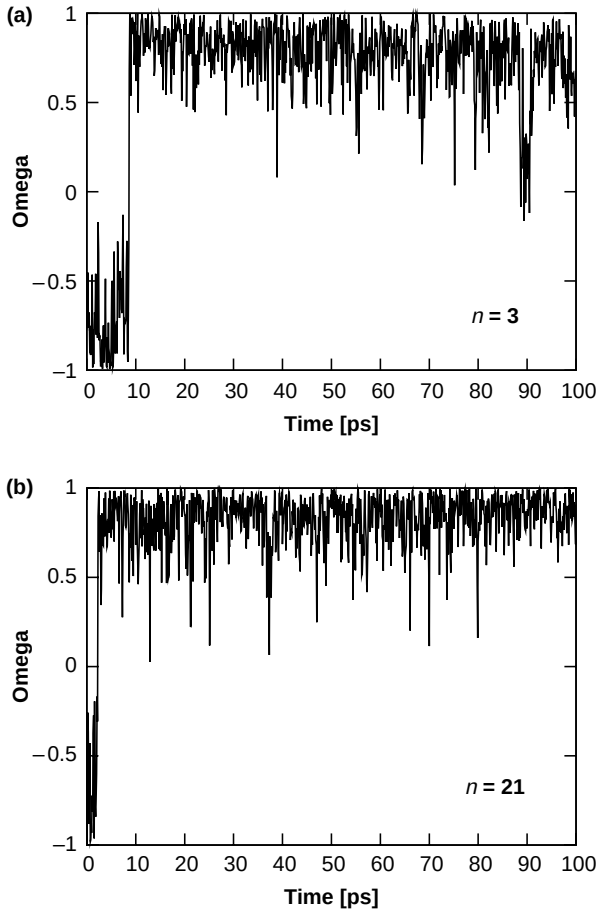

Figure 9. Orientations of molecules inside a water-filled channel. n denotes the position at the nth binding site inside the channel, starting from the molecules nearest the N-terminus. The dipoles tend to line up in a parallel fashion.

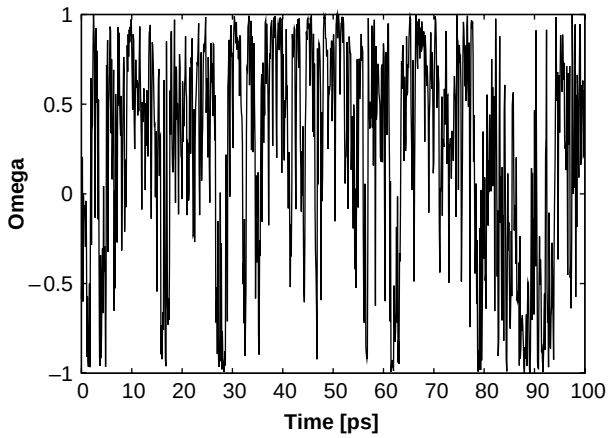

Figure 10. The orientation of one single water molecule in the channel. Transient changes in the orientation from $\Omega = 1$ to $\Omega = -1$ coincide with changes in positions.

influence of the periodic potential on the dipoles is not apparent. For comparisons, we have also considered the case of a single water molecule inside the channel. The trajectory is shown in Figure 8(b). It is interesting to note that there is a correlation between orientational and positional changes. Most of the time a positive orientation, $\Omega > 0$ is preferred, but at the moment the molecule moves, its orientation changes transiently to $\Omega = -1$ (Figure 10). This seems to be a general feature of water translocation in this type of protein channel and has been observed also in the KcsA potassium channel during MD simulations [27].

3.2 Ion-filled channel

In the following, we consider the case of a channel containing only potassium ions at various densities. The trajectories of the ions are shown in Figure 11 for three different occupation numbers: a single ion, $\nu = 3$ and $\nu = 2.182$.

Figure 11(a) shows the trajectory of a single ion. In this case, the ion does not perform long-range diffusion, which indicates that the potential barriers imposed by the carbonyls are larger than the driving force exerted by the potential gradient (Figure 4) originating from the electric field between the N- and C-termini.

Figure 11(b) shows the trajectories of nine ions embedded equidistantly in 25 binding sites ($\nu = 3$). As expected, the Coulomb repulsion among the commensurably distributed ions keeps the ions at rest in their binding sites. The thermal fluctuations are too small to move the ions along the potential gradient (Figure 4) towards the C-terminus.

Figure 11(c) shows an example of the incommensurable case. Twelve ions are located in 25 binding sites ($\nu = 2.182$). See Figure 7(b) for an illustration of this situation. Initially all have the same inter-ionic distance, separated by one binding site (vacancy), except for the two lowest ions, which have two vacant binding sites in between, i.e. one 'additional vacancy'. Therefore, the lower ions seek to accomodate their Coulomb repulsion with the periodicity of the carbonyl potential. Accordingly, the ions have a tendency to move towards the C-terminus because of the potential gradient (Figure 4). This leads to a rearrangement and hopping of the ions such that the additional vacancy moves from the bottom towards the middle of the channel where it performs random hoppings about its equilibrium positions in this region. The corresponding trajectory of the additional vacancy is shown in Figure 12. It is important to point out that in the case of only ions inside the channel and under the incommensurable condition $\nu = 2.182$, there is no long-ranged unidirectional motion of the vacancy, but rather an equilibration. This is of importance with respect to the case where all vacancies, except of the additional one, are replaced by water molecules. This situation is considered in Section 3.4.

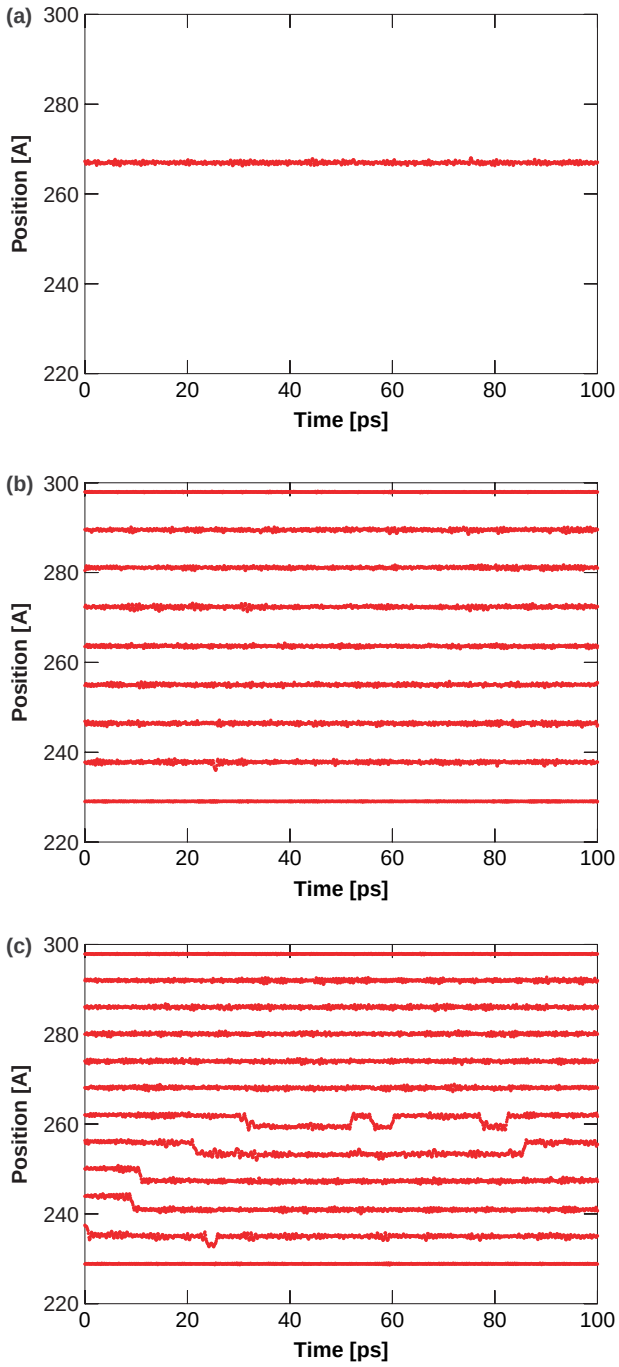

Figure 11. Trajectories of ions in a channel. (a) A single ion inside the channel, (b) occupation number $\nu = 3$ (25 binding sites) and (c) occupation number $\nu = 2.182$ (25 binding sites).

3.3 *Movements of ion–water pairs*

In the following section, we consider the situation where both ions and water molecules occupy the binding sites of the channel. In particular, we consider situations where the initial configurations consist of ion–water pairs separated by one or more vacancies. Two typical cases of trajectories are shown in Figure 13. In the dilute commensurable case

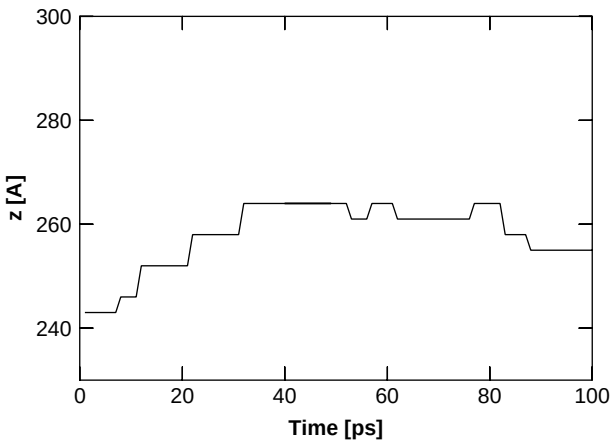

Figure 12. Trajectories of vacancy system shown in Figure 11(c).

with occupation number $\nu = 8$ (Figure 13(a)), the ion–water pairs remain in their bound state and move together with no preferred direction. Similar behaviour is observed also for the incommensurable case, $\nu = 5.75$ (Figure 13(b)), where the ions are forced to move. In fact, the hopping of the

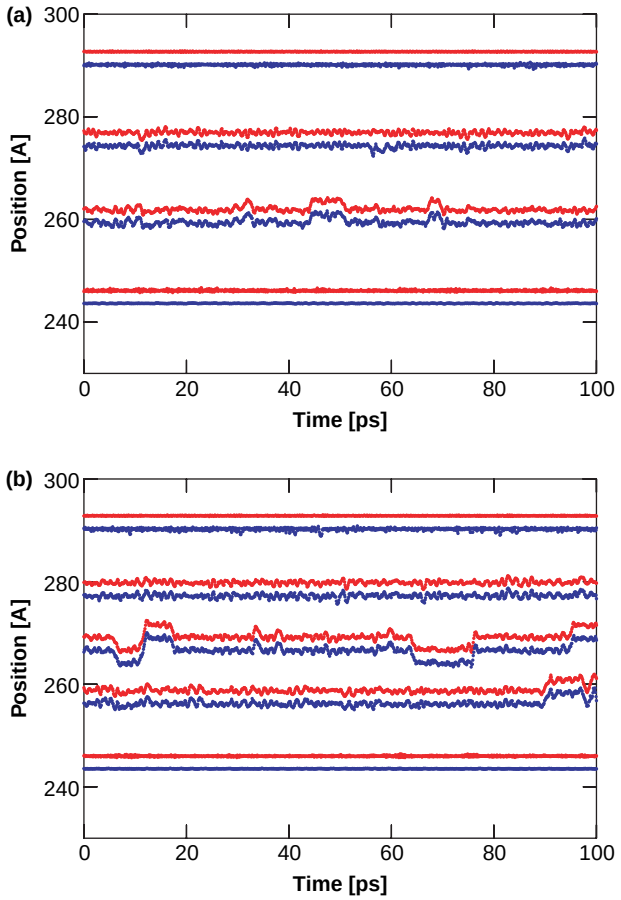

Figure 13. Trajectories of ion–water pairs. (a) Dilute commensurable case, $\nu = 8$ (25 binding sites) and (b) incommensurable case, $\nu = 5.75$ (24 binding sites).

ion–water pairs are more frequent when compared with the commensurable case, but the integrity of the bound state of the ion–water pairs is not destroyed. The appearance of a stable bound state of ion–water pairs is an important feature of this nanochannel. One reason for the stability of the ion–water pair is their Coulomb attraction. The potential energy $U(\Delta z)$, consisting of Coulomb and van der Waals interactions, between an ion and a water molecule as a function of their distance $\Delta z = z_{\text{water}} - z_{\text{ion}}$ is shown in Figure 14. The potential exhibits energy minima at a characteristic distance ≈ 3 Å for all orientations of the water molecule (bound states). The absolute minimum (polarised bound state) ≈ -18 kcal/mol ($30\,k_BT$) is located at $\Delta z = -2.7$ Å for an orientation of the water molecule that is most favourable, i.e. $\Omega = 1$. A second reason for the stability of an ion–water pair is the linear size of the binding site: the minimum of the ion–water attraction at $\Delta z = -2.7$ Å practically matches with the periodicity, ≈ 3 Å, of the lattice potential formed by the carbonyl groups of the nanochannel. Therefore, the bound state of an ion–water pair is provided by the lattice potential while resting at their binding sites, and maintained during a hopping event by their Coulomb attraction.

3.4 *Channel filled with ion–water pairs*

We consider the situation where the nanochannel is almost fully occupied with potassium ions and water in an alternating sequence. Only one vacancy is introduced near the C-terminus of the channel, as shown in Figure 2. Using the standard parameters, MD simulations were performed for 100 ps. In order to improve the statistics, the simulations were performed 10 times, using different seed numbers for each simulation. The trajectories of the potassium ions and the water molecules of one example of the simulations are shown in Figure 15. The ions and water molecules exhibit a long-range unidirectional motion from the N-terminus towards the C-terminus (from top to bottom) of the nanochannel. A closer inspection of the trajectories indicates that the movements of ions and water molecules take place as hopping events of ion–water pairs. This is more easily observed by analysing the trajectory of the single vacancy in the system (Figure 16(a)). There the vacancy exhibits hopping processes over distances equal to or larger than two binding sites (≈ 6 Å) within a time window of 0.1 ps. This implies that the conduction of ions in the channel takes place by the hopping of ion–water pairs. The example of simulation shown in Figures 15 and 16(a) is not an anecdotal event; however, the mean drift of the single vacancy averaged over 10 independent runs, which is depicted in Figure 16(b), confirms the long-range drift of the vacancy. It should be noted that the effects of the energy barriers at the mouth regions and the outer bath has not been particularly addressed in the present studies. However, it can be expected that the ion–water transport, as observed in Figure 16, is affected to a small extent only by the boundary conditions at the beginning and at the end of the trajectories.

The important role of water during the hopping processes can be inferred by the comparison of the trajectories shown in Figures 15 and 11(c). In both cases, the ion occupation number is $\nu = 2.18$, but in the latter case the ions have to move without water molecules. Comparing the corresponding trajectories of the particular vacancy, Figures 16(a) and 12, it clearly shows that without the support of water molecules the ions do not perform a long-range drift along the nanochannel. The reasons for that are not well understood. One possibility is that the long-range polarised state of the water molecules (Figure 9) plays a role.

Another possibility is the hypothesis that a water molecule may act as 'pawl' in a ratchet mechanism [38].

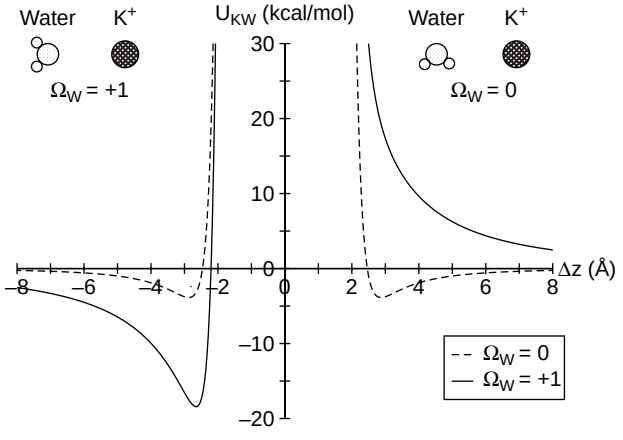

Figure 14. The interaction energy between a K^+ ion and a water molecule with different orientations Ω_W as a function of their relative position $\Delta z = z_{\text{water}} - z_{\text{ion}}$. The 'polarised bound state' of $\Omega = 1$ at 2.65 Å has an energy of -18.08 kcal/mol ($30\,k_BT$).

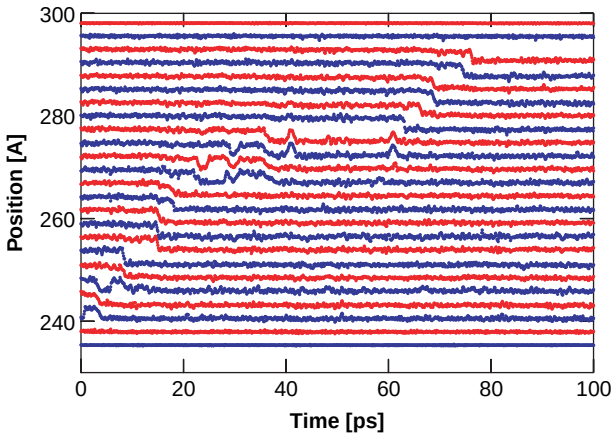

Figure 15. Trajectories for ions (red) and water (blue) at $\nu = 2.18$ (25 binding sites).

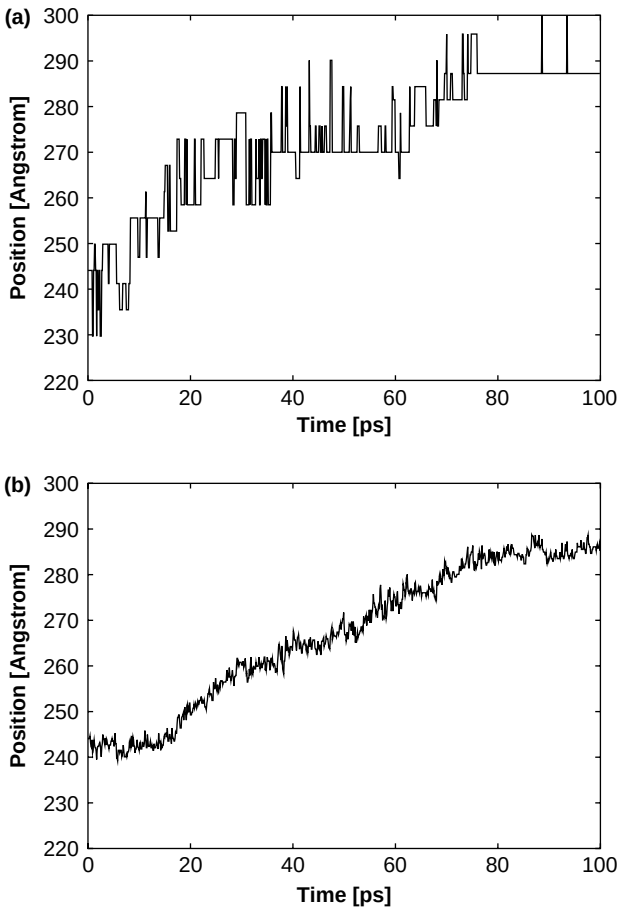

Figure 16. (a) Trajectory of the vacancy corresponding to Figure 15. (b) Average trajectory of the vacancy of 10 independent runs.

Let us consider this mechanism in a simple pair approximation picture where we assume that the ion–water pair hops as a stable entity by one binding site. The initial configuration is depicted in Figure 2, and we denote the sequence from bottom to top by W_1, K_2, W_3, vacancy$_4$, K_5, W_6, K_7, etc. In this situation, the water W_3 can be assumed to have the tendency to be polarised by K_2 with $\Omega \approx -1$ due to the lack of a neighbouring ion at site 4, and forms a stable polarised bound state with K_2 (permon). The interaction of the pair K_2–W_3 with the ion K_5 is repulsive. If solely W_3 would hop to the vacant site 4, it would have to change its orientation to $\Omega \approx +1$, which corresponds to an energy barrier of $\approx 30\,k_BT$ (Figure 14). Therefore, the hopping of this pair or W_3 towards the vacancy is less probable. Since W_3 is essentially responsible for this prohibition, it may be considered as a 'pawl' in this ratchet model. The situation for the opposing pair K_5–W_6, however, is different. Due to the influence of K_5 and K_7 on W_6, this water molecule has orientations fluctuating around $\Omega \approx 0$ forming transiently bound pairs of K_5–W_6 and W_6–K_7. Influenced by the gradient of the channel potential (Figure 4), the movements of the ion K_5 are biased towards the vacancy. Therefore, if the transiently formed permon K_5–W_6 with $\Omega \approx -1$ moves towards the vacancy, then its state becomes stabilised in the same way as the preceding pair K_2–W_3. From this new situation, the whole process as described above will take place again for K_7–W_8 and so on. This leads to the unidirectional movements of ions and water in the nanochannel. It should be noted that the described hypothetical ratchet model for the correlated movements of ions and water is different from the variety of ratchet models discussed in the literature (see [39–43]). Almost all ratchet models rely on the principle that the directed motion of particles in spatially periodic structures under the influence of a weak external (constant or periodic) force can be induced if the periodic potential or the fluctuations are asymmetric. A typical example of such a ratchet model is the overdamped Langevin equation of a single particle at coordinate $x(t)$

$$\eta \frac{dx}{dt} = -\frac{dU}{dx} + F + \xi(t), \tag{0.3}$$

where $\xi(t)$ is a Gaussian white noise of zero mean, F is a constant homogeneous force and $U(x)$ is a periodic asymmetric potential (e.g. an asymmetric sawtooth potential). This is different from the present model where the asymmetry is related to the 'particle' itself (ion–water pair with water acting as a pawl), rather than to the fluctuating channel potential $U(x)$, which is on average spatially symmetric. The formulation of this model corresponding to Equation (0.3) is a formidable task.

One important aspect that differs from other one-dimensional ion conductors, e.g. superionic conductors [19–24], is the dynamic nature of the lattice potential. The flexibility of the carbonyl groups, which represent a periodic one-dimensional, fluctuating lattice potential for ions and water molecules, has a significant influence on the movements of the occupants in the channel. This can be demonstrated by the particular situation where the thermal fluctuations of the whole protein are essentially frozen. Employing a spring constant of 100.0 kcal/mol Å^2 for all atoms of the protein, this provides approximately a static potential for ions and water. Apart from the constraints on the channel, all other simulation parameters were kept the same as in the other simulations. Figure 17 shows the corresponding trajectories of the occupants within the channel. It is observed that the static potential prohibits any movements of the occupants, i.e. the potential barriers imposed by the carbonyl atoms are higher than the inter-ionic Coulomb repulsion. Even a widening of the channel to a diameter of 8 Å, in order to lower the potential barriers, do not promote a diffusion of ions and water, but rather increases the displacements of them. A further increase in the diameter is not useful, because higher channel diameters would change the validity of a strict one-dimensional model by allowing the occupants to pass

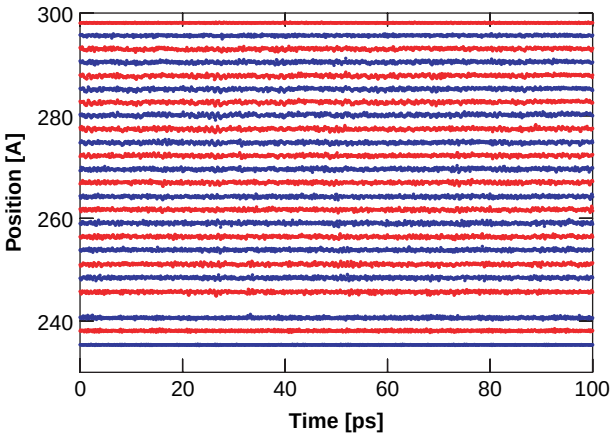

Figure 17. Trajectories of K^+ (red) and water (blue) during a simulation with rigid channel constraints. The potential barrier is high enough to prevent any movement.

each other. The effects of the dynamics of the carbonyls on the movements of ions and water have been addressed recently in more detail [27,28].

4. Summary and conclusions

We have studied the molecular mechanism of ion transport in a long channel filled with an alternating sequence of ions and water molecules at various densities by MD simulations. It was shown that the ion conductivity is based on a concerted movement of the three constituents of the channel: the ions, the water molecules and the flexible carbonyl groups of the channel's backbone. Previous predictions [28] are confirmed and support the theory that the unidirectional transport is based on cooperative hopping processes of bound ion–water pairs mediated by the adjustable lattice potential of the carbonyls (permons). It was shown that isolated ion–water pairs do not perform long-ranged movements, but perform localised hopping as quasi-entities. At higher densities, ion–water pairs exhibit a long-ranged drift. It is argued that the water molecules cause a rectification of the movements of ion–water pairs at high densities.

The presented results are thought to provide the molecular basis of a mathematical theory of ion conduction in the channels of the type presented in this paper, and for ion conduction in biological potassium channels [27]. This, however, has still to be done. It is still not clear whether this theory will be based on a ratchet-type theory [41,43], or it will follow a quasi-particle concept as it is common in solid-state physics [44] and which has been suggested recently for ion channels [8].

Note

1. Present address: Research Center for Applied Sciences, Academia Sinica, Taipei 11529, Taiwan, R.O.C.

References

[1] T. Chou and D. Lohse, *Entropy-driven pumping in zeolites and biological channels*, Phys. Rev. Lett. 82 (1999), pp. 3552–3555.
[2] D. Dubbeldam, S. Calero, T.L.M. Maesen, and B. Smit, *Incommensurate diffusion in confined systems*, Phys. Rev. Lett. 90 (2003), 245901.
[3] A. Kalra, S. Garde, and G. Hummer, *Osmotic water transport through carbon nanotube membranes*, Proc. Natl Acad. Sci. USA 100 (2003), pp. 10175–10178.
[4] I.-C. Yeh and G. Hummer, *Nucleic acid transport through carbon nanotube membranes*, Proc. Natl Acad. Sci. 101 (2004), pp. 12177–12182.
[5] Y. Fujiyoshia, K. Mitsuoka, B.L. de Groot, A. Philippsen, H. Grubmüller, P. Agre, and A. Engel, *Structure and function of water channels*, Curr. Opin. Struct. Biol. 12 (2002), pp. 509–515.
[6] J.H. Morais-Cabral, Y.F. Zhou, and R. MacKinnon, *Energetic optimization of ion conduction rate by the k^+ selectivity filter*, Nature 414 (2001), pp. 37–42.
[7] S. Berneche and B. Roux, *A microscopiv view of ion conduction through the k+ channel*, Proc. Natl Acad. Sci. 100 (2003), pp. 8644–8648.
[8] R. Elber, D.P. Chen, D. Rojewska, and R. Eisenberg, *Sodium in gramicidin: An example of a permion*, Biophys. J. 68 (1995), pp. 906–924.
[9] D.A. Doyle, J. Morais-Cabral, R.A. Pfuetzner, A. Kuo, J.M. Gulbis, S.L. Cohen, B.T. Chait, and R. MacKinnon, *The structure of the potassium channel: molecular basis of k^+ conduction and selectivity*, Science 280 (1998), pp. 69–77.
[10] Y.F. Zhou, J.H. Morais-Cabral, A. Kaufman, and R. MacKinnon, *Chemistry of ion coordination and hydration revealed by a k^+ channel-fab complex at 2.0Å resolution*, Nature 414 (2001), pp. 43–48.
[11] B. Hille, *Ion Channels of Excitable Membranes*, 3rd ed., Sinauer Associates Inc., Sunderland, MA, 2001.
[12] A.L. Hodgkin and R.D. Keynes, *The potassium permeability of a giant nerve fibre*, J. Physiol. 128 (1955), pp. 61–88.
[13] T.W. Allen, S. Kuyucak, and S.-H. Chung, *Molecular dynamics study of the kcsa potassium channel*, Biophys. J. 77 (1999), pp. 2502–2516.
[14] S. Bernéche and B. Roux, *Molecular dynamics of the kcsa k^+ channel in a bilayer membrane*, Biophys. J. 78 (2000), pp. 2900–2917.
[15] I.H. Shrivastava and M.S.P. Sansom, *Simulations of ion permeation through a potassium channel: molecular dynamics of kcsa in a phospholipid bilayer*, Biophys. J. 78 (2000), pp. 557–570.
[16] S.-H. Chung, T.W. Allen, and S. Kuyucak, *Conducting-state properties of the kcsa potassium channel from molecular and brownian dynamics simulations*, Biophys. J. 82 (2002), pp. 628–645.
[17] S. Kuyucak, O.S. Andersen, and S.-H. Chung, *Models of permeation in ion channels*, Rep. Prog. Phys. 64 (2001), pp. 1427–1472.
[18] B. Roux, T. Allen, S. Berneche, and W. Im, *Theoretical and computational models of biological ion channels*, Quart. Rev. Biophys. 37 (2004), pp. 15–103.
[19] J.C. Wand and D.F. Pickett, *One-dimensional models for superionic conductors*, J. Chem. Phys. 65 (1976), pp. 5378–5384.
[20] J.B. Sokoloff, *Ionic order and defect conductivity in the one-dimensional superionic conductor hollandite*, Phys. Rev. B 17 (1978), pp. 4843–4849.
[21] T. Geisel, *Interacting brownian particles and correlations in superionic conductors*, Phys. Rev. B 20 (1979), pp. 4294–4302.
[22] H.U. Beyeler, L. Pietronero, and S. Strässler, *Configurational model for a one-dimensional ionic conductor*, Phys. Rev. B 22 (1980), pp. 2988–3000.
[23] M. Weiss and F.-J. Elmer, *Dry friction in the frenkel-kontorova-tomlinson model: static properties*, Phys. Rev. B 53 (1996), p. 7539.
[24] Y. Michiue and M. Watanabe, *Atomistic simulation study of k-hollandite: Ionic correlation and dynamics of the linearly disordered solid*, Phys. Rev. B 59 (1999), pp. 11298–11302.
[25] J. Piasecki, R.J. Allen, and J.-P. Hansen, *Kinetic models of ion transport through a nanopore*, Phys. Rev. E 70 (2004), 021105.

[26] H. Lu, J. Li, X. Gong, R. Wan, L. Zeng, and H. Fang, *Water permeation and wavelike density distributions inside narrow nanochannels*, Phys. Rev. B 77 (2008), p. 174115.
[27] J.F. Gwan and A. Baumgaertner, *Cooperative transport in a potassium ion channel*, J. Chem. Phys. 127 (2007), p. 045103.
[28] J.F. Gwan and A. Baumgaertner, *Ion transport in a nanochannel*, J. Comput. Theor. Nanosci. 4 (2007), pp. 50–56.
[29] Y. Zhou and R. MacKinnon, *The occupancy of ions in the k^+ selectivity filter: Charge balance and coupling of the ion binding to a protein conformational change undelie high conduction rates*, J. Mol. Biol. 333 (2003), pp. 965–975.
[30] W.L. Jorgensen, J. Chandrasekhar, J.D. Madura, R.W. Impey, and M.L. Klein, *Comparsion of simple potential functions for simulating liquid water*, J. Chem. Phys. 79 (1983), pp. 926–935.
[31] D.A. Case, D.A. Pearlman, J.W. Caldwell, T.E. Cheatham, W.S. Ross, C. Simmerling, T. Darden, K.M. Merz, R.V. Stanton, A. Cheng et al., *AMBER 5.0*, University of California, San Francisco, 1997.
[32] M. Haan, *Simulations of a biological ion channel*, MSc thesis, University Duisburg-Essen, Duisburg, Germany, 2007.
[33] H.J.C. Berendsen, J.P.M. Postma, W.F. van Gunsteren, A. DiNola, and J.R. Haak, *Molecular dynamics with coupling to an external bath*, J. Chem. Phys. 81 (1984), pp. 3684–3690.
[34] S.J. Weiner, P.A. Kollman, D.T. Nguyen, and D.A. Case, *An all atom force field for simulations of proteins and nucleic acids*, J. Comp. Chem. 7 (1986), pp. 230–252.
[35] A. Onufriev, D. Bashford, and D.A. Case, *Modification of the generalized born model suitable for macromolecules*, J. Phys. Chem. B 104 (2000), pp. 3712–3720.
[36] J. Srinivasan, M.W. Trevathan, P. Beroza, and D.A. Case, *Application of a pairwise generalized born model to proteins and nucleic acids: inclusion of salt effects*, Theor. Chem. Acc. 101 (1999), pp. 426–434.
[37] J. Frenkel and T. Kontorova, *On the theory of plastic deformation and twinning*, J. Phys. (Moscow) 1 (1939), pp. 137–149.
[38] R. Feynman, R. Leighton, and M. Sands, *The Feyman Lectures on Physics*, Vol. 1, Addison Wesley, Reading, MA, 1963.
[39] R.D. Vale and F. Oosawa, *Protein motors and maxwell's demons: Does mechanochemical transduction involve a thermal ratchet?* Adv. Biophys. 26 (1990), pp. 97–134.
[40] A. Adjari and J. Prost, *Mouvement induit par un potentiel periodique de basse symetrie: dielectrophorese pulsee*, C.R. Acad. Sci. Paris II 315 (1992), pp. 1635–1639.
[41] M.O. Magnasco, *Forced thermal ratchets*, Phys. Rev. Lett. 71 (1993), pp. 1477–1480.
[42] R.D. Astumian, *Thermodynamics and kinetics of a brownian motor*, Science 276 (1997), pp. 917–922.
[43] P. Reimann and P. Hänggi, *Introduction to the physics of brownian motors*, Appl. Phys. A 75 (2002), pp. 169–178.
[44] P.W. Anderson, *Concepts in solids: Lectures on the Theory of Solids*, 2nd ed., W.A. Benjamin, Reading, MA, 1971.